VCSEL-based Radio-over-G652 Fiber System for short/medium range MFH solutions

Jacopo Nanni, Jean-Luc Polleux, Catherine Algani, Simone Rusticelli, Federico Perini, Giovanni Tartarini

***Abstract*—In view of the realization of short and medium range Mobile Front-Haul (MFH) connections for present (LTE) and future (5G) cellular networks, a cost effective, low consumption Radio over Fiber system is proposed, based on 850 nm Single Mode Vertical Cavity Surface Emitting Lasers (VCSELs) and Standard Single Mode Fibers (SSMFs). An efficient countermeasure to possible impairments due to the bi-modal behavior of SSMFs at 850 nm allows even in critical cases to maintain at high level the quality of the received signal. The performances are evaluated with reference to the Physical Downlink Shared Channel of an entire LTE frame with 20 MHz bandwidth centered in band 20 of the standard. In terms of Error Vector Magnitude and outage probability under temperature stress the system is able to transmit 256-QAM signals in compliance with the LTE standard, which corresponds to a raw data rate transmission of 134.4 Mbit/s, up to distances of 1.5 km.**

***Index Terms*—Optical fiber communication; Surface-emitting lasers; Microwave communication.**

I. Introduction

A feature which is observed in nowadays 4G architectures of Radio Access Networks (RANs) and is expected for the future 5G ones is the separation of the digital processing/management sections from the radio access ones reaching the end users (see Fig. 1). Indeed in this way the former, which can have different denominations, like BBU (Baseband Unit) or DU (Digital Unit) section, can be centralized, which leads to a reduction of the related installation and maintenance costs and to an improvement of spectral efficiency through the adoption of appropriate cooperative algorithms . In addition, this makes it possible to realize functionalities like Network Function Virtualization (NFV) and Software Defined Networking (SDN) [1]–[3].

As a consequence of this architecture, the Radio Access section can be constituted by large amounts of elements, which are typically indicated as Remote Radio Units/Heads (RRUs/RRHs), Remote Antenna/Access Units (RAUs), or also Radio Dots (RD), deployed with high capillarity and guaranteeing a high performance traffic available at each of the corresponding cells [4]. The Very Dense Network (VDN) which is created by this architecture, results to be based on the Distributed Antenna System (DAS) concept, which allows to provide high capacity while minimizing cost and power consumption [5], [6].

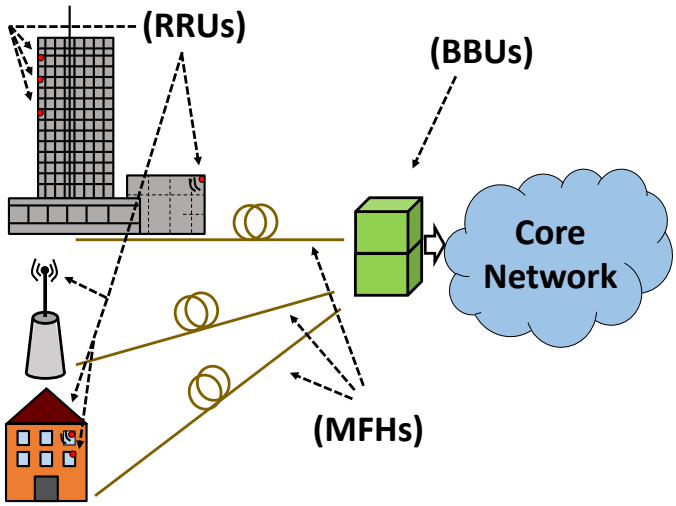

Fig. 1: Example of centralized architecture of Radio Access Network (RRU: Remote Radio Unit; MFH: Mobile Front Haul; BBU: Baseband Unit).

Among the possible technologies adopted to realize the Mobile Front-Haul (MFH), which connects RRUs and BBUs (see again Fig. 1), Analog Radio over Fiber (A-RoF) is one of the most promising. Important advantages related to its adoption are indeed the low complexity required at the RRU stages, and the low requirements in terms of link throughput [7]. Thanks to these features the A-RoF technology constitutes a consolidated optimal solution for the coverage in non Line of Sight (LoS) and/or crowded environments, such as shopping malls, stations, stadiums, etc., and can also be efficiently exploited for the realization of MFHs in alternative or in cooperation with the Digital Radio over Fiber (D-RoF) technique, on which protocols like the Common Public Radio Interface (CPRI) or the Open Base Station Architecture Initative (OBSAI) are based [8]–[13].

Focusing on the infrastructure of VDNs, huge numbers of network cells and consequently of MFHs have to be realized, making it mandatory to decrease as much as possible cost and consumption of each A-RoF link [14]. In this perspective, Vertical Cavity Surface Emitting Lasers (VCSELs) operating at the wavelength $\lambda \simeq 850\,nm$ have been demonstrated as very attractive candidates to be implemented for telecommunication

J. Nanni and G.Tartarini are with the Dipartimento di Ingegneria dell'Energia Elettrica e dell'Informazione "Guglielmo Marconi", Università di Bologna, 40136 Bologna, Italy (e-mail: jacopo.nanni3@unibo.it; giovanni.tartarini@unibo.it).

J.L.Polleux is with Université Paris-Est, ESYCOM (EA2552), ESIEE Paris, UPEM, Le Cnam, 93162 Noisy-le-Grand, France (e-mail: jean-luc.polleux@esiee.fr; carlos.viana@esiee.fr).

C.Algani is with Le Cnam, ESYCOM (EA2552), 75003 Paris, France (e-mail: catherine.algani@cnam.fr).

F.Perini and S.Rusticelli are with Institute of Radio Astronomy, National Institute for Astrophysics, Via Fiorentina 3513, 40059 Medicina, Italy (e-mail: f.perini@ira.inaf.it;rusticel@ira.inaf.it).

systems. It should therefore be investigated their capability to replace Distributed FeedBack (DFB) lasers, which are historically the most employed optical sources in A-RoF systems, operating in second ($\lambda \simeq 1310\,nm$) and third ($\lambda \simeq 1550\,nm$) optical windows.

Indeed, it is well-known how GaAs VCSEL operating at $\lambda \simeq 850\,nm$ can reach threshold currents of very few mA ($\sim 8-10$ times less than common DFB laser) keeping the conversion efficiency high. Moreover, due to the very small size and vertical behavior, the manufacturing costs are low with respect to edge emitting lasers [15] while the circular beam shape which comes out from the vertical structure facilitates coupling with optical fibers. Presently, one of the major application of VCSELs for telecommunications regards baseband data transmission and is implemented in data center where Multi-Transverse-Mode (MTM) VCSELs are used together with standard Multimode Fibers (MMFs) for distances of few meters [16]–[19]. Regarding A-RoF transmission, VCSEL-based optical links have been proposed, especially for short distances communications in DAS applied for example in Gigabit Wi-Fi for Home Area Network (HAN) [20] [21].

With the aim to further increase the performance-to-cost ratio, it is of interest to consider the use of Standard Single Mode Fiber (SSMF) as optical transmission channel, still keeping VCSEL operating at $\lambda \simeq 850$ nm. The main reason lies in lower cost of SSMF with to respect MMF in terms of manufacturing processes [22], together with the possibility of exploiting already existing SSMF-based infrastructures. The drawback of using SSMF at $\lambda \simeq 850$ nm is the bi-modal behavior of the fiber [23] which produces notches in the modulation bandwidth where the number and spacing between them are proportional to the length of the fiber span.

A possible solution to the problem could be to use long wavelength VCSELs (generally made in quaternary composition) which emit at $\lambda \simeq 1310\,nm$ or $\lambda \simeq 1550\,nm$, where the SSMF operates in single-mode regime. This could be a solution for long-distance MFHs [24], thanks also to the lower attenuation exhibited by the fiber in the second and third optical windows with respect to the first one. However, the higher cost and lower reliability of these VCSELs compared to binarily-composed $\lambda \simeq 850\,nm$ ones [25], lowers the level of convenience of this choice for MFHs of reduced length (to give a reference value, say up to around $1\,km$), for which fiber attenuation does not constitute a major problem.

For the realization of short- and medium- range MFH it is then proposed in this paper a solution which utilizes VCSEL sources operating in the first optical window together with SSMF fibers. The solution consists in introducing between VCSEL source and SSMF strand a short span of truly-single mode fiber at $\lambda \simeq 850\,nm$ as initial pigtail. This introduction, which showed to reduce the possible fluctuations of the received RF power due to modal noise [26], is here presented as a technical feature of 850 nm-VCSEL-based Radio-over-SSMF links, keeping to an acceptable level the impairments due to modal noise, and also those due to intermodal dispersion. This allows to appreciate the adoptability of this low-cost, low-consumption ARoF solution in the realization of VDNs of present and next generation.

The paper, which extends the work presented in [27], is organized as follows. A description of the bench setup is firstly presented, showing the characterization of each component of the proposed system. Then, the main performances of the system itself are presented in terms of Error Vector Magnitude (EVM) and outage probability, showing compliance with the LTE standard.

II. A-RoF System and Measurement Setup

The experimental setup utilized in the present work is represented in Fig 2 and comprises substantially three main parts: a first one, composed by an off-line LTE frame generator and by a Vector Signal Generator (VSG), which generates an LTE signal, a second one, which is an A-RoF system transmitting such signal, and a third one, composed by a Vector Signal Analyzer (VSA) followed by an off-line LTE frame receiver, which studies the characteristics of the received signal.

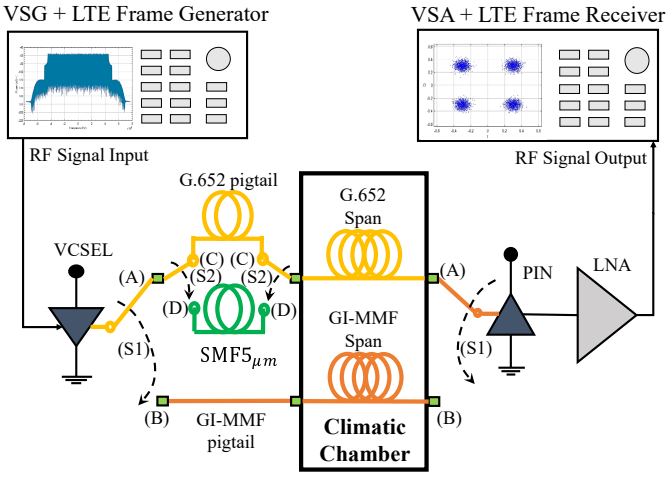

Fig. 2: Analog Radio over Fiber systems considered and corresponding measurement setup.

The core of the whole experimental bench is the A-RoF system, whose optical transmitting section consists of a directly modulated laser operating at $850\,nm$. In the system proposed, the laser is a single mode (SM) VCSEL, and the fiber span consists of a strand of SSMF (G.652 type). This means that the switch S1 of Fig. 2 is in position A. Another symbolical switch (S2) is represented in Fig. 2 to illustrate two possible configurations of the proposed system. In the first, where S2 is in position C, a short pigtail of G.652 fiber connects the SM VCSEL to the G.652 strand. In the second (position D) the connection with the G.652 strand is obtained introducing a truly-single mode fiber at $\lambda \simeq 850\,nm$ as initial pigtail. This fiber exhibits a core diameter of about $5\,\mu m$ and will be indicated as SMF$_{5\,\mu m}$. The fiber strands, either SSMF or GI-MMF, determine the link length and are placed inside a climatic chamber, where a ramp of temperature variation can be imposed. This allows to test the performances of the RoF link in presence of environmental variations, determining a statistical time variation of the EVM and the

outage probability of the system. Finally, at the fiber end section, a GaAs PIN photodetector is present, followed by a low consumption Low Noise Amplifier (LNA). Note that no feedback loop was employed for temperature stabilization of the SM VCSEL, since the environment temperature was not undergoing sharp variations. As mentioned above, the first part of the experimetal setup generates the LTE signal which is given in input to the A-RoF system. The practical situation emulated is an FDD downlink LTE frame transmission, which is realized compliantly with the release 13 of the standard [28]. In particular, the entire frame of 10 ms duration is created offline using a locally developed MATLAB software which generates the samples and then uploads them to the VSG. The VSG in turn creates the modulating signal and up-converts it to the wanted RF carrier frequency through an internal oscillator, in order for it to be launched into the RoF link under test. After the A-RoF link the signal is received by the VSA, which down-converts the received bandpass signal, making the received data available to perform an off-line post processing. This operation is again performed through an ad-hoc locally developed MATLAB software, which is able to synchronize the frame, equalize the channel and extract the EVM for each physical and logical channel of the transmitted signal.

The LTE signal chosen exhibited a bandwidth of 20 MHz and a measured Peak-to-Average Power Ratio (PAPR) of about 10.5 dB in the back-to-back configuration. The link characterization was performed with particular reference to band 20 of the LTE standard (frequency carrier $f_c = 800\,MHz$). With reference to the A-RoF system proposed, the measured PAPR in band 20 for different RF input powers is reported as inset in Figure 3b. However, its performance was also tested for other values of f_c, ranging in the interval $f_c \in [500, 1000]\,MHz$. Indeed, this interval plays an important role in terms of applications, since it includes frequencies generally considered in LTE band 20 together with possible future frequencies for 5G [29]. This analysis put into evidence the possible onset of critical working points of the system, and allowed to illustrate the use of the $\text{SMF}_{5\,\mu m}$ pigtail represented in Fig. 2 as a possible solution. The SM VCSEL employed was furnished by Optowell. As shown in Figure 3a, it presents a threshold current $I_{th} \simeq 2\,mA$ and a maximum current before the roll-off $I_s \simeq 5\,mA$. The slope-efficiency $\eta_{TX} = \frac{dP}{dt} \simeq 0.16\,mW/mA$ can be directly extracted from Fig. 3a.

The chosen value for the biasing current of the laser was $I_{bias} = 4.5\,mA$, since it showed to give the best EVM results. Figure 3b shows the behavior of the SM VCSEL modulation response in correspondence to that working point. In line with the typical VCSEL characteristics, the series resistance (or differential resistance) in DC is around $50\,\Omega$ for the chosen value of I_{bias} (see Figure 3a). This value was measured to be same also at the modulating frequencies considered, so no matching circuit was needed. Finally, the Relative Intensity Noise (RIN) of the SM VCSEL was also measured, resulting to be around -128 dB/Hz for $f = 800\,MHz$.

As mentioned above, the usage of SSMF at 850 nm needs particular attention. In fact, it is well known [30] that for wavelengths around 850 nm, both LP_{01} and LP_{11} modes propagate in the fiber in a well above cutoff fashion, exhibiting

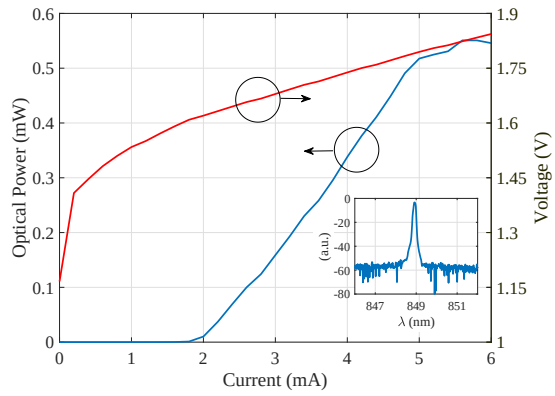

(a)

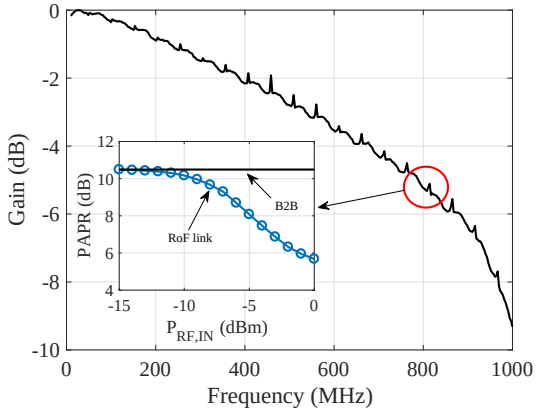

(b)

Fig. 3: (a) L-I-V characterization and (inset) optical emission spectrum of the SM VCSEL utilized. (b) Normalized Modulation response and (inset) measured PAPR at $800\,MHz$ of the proposed A-RoF system.

group delays per unit length respectively equal to $\hat{\tau}_1$ and $\hat{\tau}_2$, and giving rise to notches within the modulation bandwidth of the fiber channel, because of intermodal dispersion. Indeed, the modulation response of the fiber results to depend both on the frequency f_c of the modulating RF carrier and on the length L of the SSMF span. Assuming for simplicity that the relative weight of the two modes is almost the same, taking into account the only effects of fiber attenuation and intermodal dispersion the normalized RF power gain g is given by:

$$g = \frac{P_{RF,\,OUT}}{P_{RF,\,OUT}|_{L=0}} = 10^{-\frac{2\alpha}{10}L} \cdot cos^2\left(2\pi f_c \frac{\hat{\tau}_1 - \hat{\tau}_2}{2} L\right) \quad (1)$$

where $\alpha = 2.4\,dB/km$ is the attenuation constant of the G.652 fiber utilized, while $P_{RF,\,OUT}$ is the RF power at the receiver-end of the system. The relationship expressed by Eq. 1 determines steep reductions in the modulation response when f_c and L are in the vicinity of the values which satsfy the relationship $f_c \cdot L = (k + 1/2)\,1/|\hat{\tau}_1 - \hat{\tau}_2| \qquad k = 0, 1, 2, \ldots$.

Fig. 4 visualizes the regions in the (f_c, L) plane where, according to Eq. 1 and for the SSMF utilized in the present work, which features $|\hat{\tau}_1 - \hat{\tau}_2| = 2.38\,\frac{nsec}{km}$, g is lower

than the value of 10% taken as a reference. It can be there appreciated that in the interval $500\,MHz < f_c < 1\,GHz$, for values of L sufficiently low (e. g. $L = 70\,m$) the region corresponding to the minima of g is not touched. On the contrary, for higher values of L it is possible to observe bandwidths where one or more regions are intersected. For example, for $L = 300\,m$ such bandwidth goes roughly from $f_c = 550\,MHz$ to $f_c = 850\,MHz$. This means that the main operating frequency here utilized ($f_c = 800\,MHz$) is subjected for $L = 300\,m$ to the impairments related to the presence of a notch in the normalized RF power gain of the optical channel. These impairments actually result from a detrimental combination of intermodal dispersion and modal noise effect. Indeed, modal noise generates slow fluctuations of the received power, and, as shown in [26], the variance of the RF received signal due to modal noise reaches its maximum in the regions of minimum produced by intermodal dispersion.

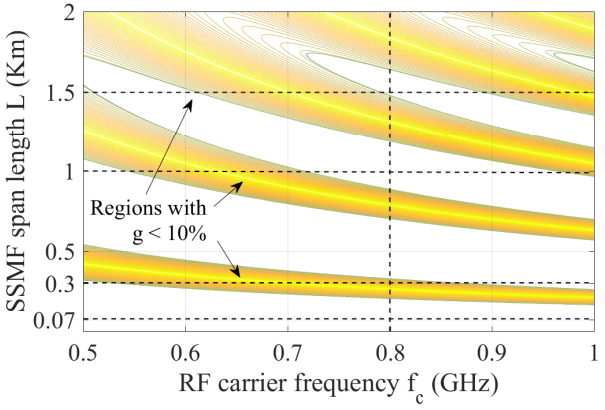

Fig. 4: Regions where normalized RF gain g is equal or lower than 10%, as a function of frequency f_c of the modulating RF carrier and length L of the SSMF span.

Finally, the receiver part of the A-RoF system depicted in Fig. 2 is composed of a GaAs PIN photodiode and a $50\,\Omega$ LNA having a gain of 20 dB and a noise figure of $2.7\,dB$ at $800\,MHz$. Note that an important characteristic of the amplifier employed is that it has a relative low current consumption ($30\,mA$), which is suitable for low cost VDN requirements.

III. Performance of the A-RoF system composed of SM VCSEL and SSMF

A. EVM characterization

In compliance with the LTE standard, the EVM computed through the off-line post-processing operations mentioned in Section II, is defined as follows:

$$EVM = \sqrt{\frac{\sum_k \left(I_k - \tilde{I}_k\right)^2 + \left(Q_k - \tilde{Q}_k\right)^2}{\sum_k I_k^2 + Q_k^2}} \qquad (2)$$

where, referring to the k-th symbol of the Physical Downlink Shared Channel (PDSCH), I_k, Q_k and $\tilde{I}_k$, $\tilde{Q}_k$ are the phase and quadrature components of the transmitted and received k-th symbol respectively.

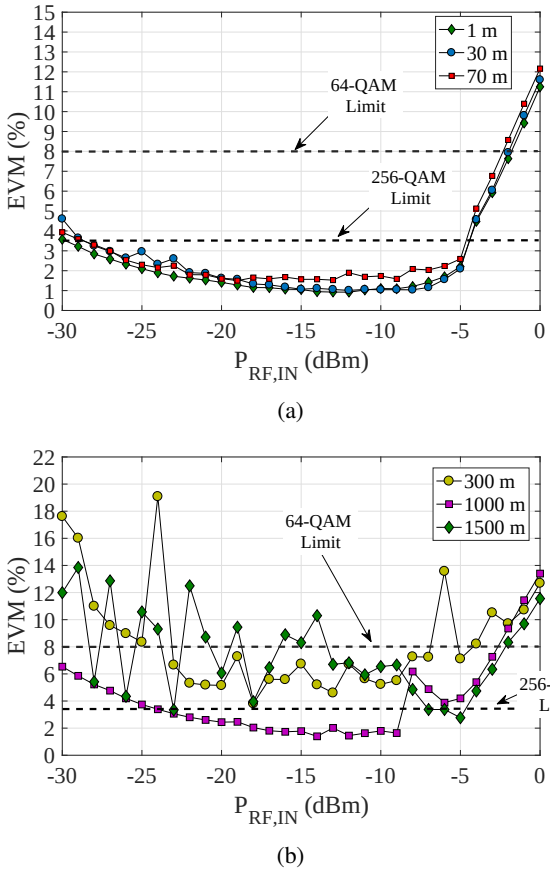

Fig. 5: EVM Measurements of short-range (up to $70\,m$) (a) and medium-range (up to $1500\,m$) (b) A-RoF systems.

Fig. 5a and Fig. 5b show EVM results for varying values of the input RF power $P_{RF,IN}$ respectively for short range (up to $70\,m$) and for medium-range (from $300\,m$ to $1500\,m$) link connections.

The A-RoF system utilized was the one depicted in Fig. 2 with the symbolical switches S1 and S2 in positions A and C, respectively, i.e. only fiber of G.652 type is placed after the VCSEL source.

For all the lengths reported in Fig. 5a the performance required in [31] for 256-QAM transmission is satisfied for input RF powers up to about $P_{RF,IN} \simeq -5\,dBm$ (and up to $P_{RF,IN} \simeq -2\,dBm$ for 64-QAM). Among the medium-range distances a similar performance is observed for $L = 1\,km$, while this does not happen for $L = 300\,m$ because,as noted with reference to Fig. 4, at this distance the modulation frequency of $800\,MHz$ is affected by the combined effect of intermodal dispersion and modal noise. For $L = 300\,m$ the EVM exhibits indeed an unstable behavior versus $P_{RF,IN}$ often exceeding the threshold value referred to 256-QAM and even 64-QAM transmission. Still from Figure 5b a similar behavior can be observed for $L = 1.5\,km$, and looking again at Figure 4 the behavior can be ascribed to the same physical reason adduced for $L = 300\,m$. Indeed, the point

corresponding to $L = 1.5\,km$ and $f_c = 800\,MHz$ results to be in the vicinity of the region where g exhibit very low values. Therefore the detriments due to the combined effect of modal dispersion and modal noise affect the received signal also in this case.

B. Outage probability under forced temperature variations

To observe the performance of the A-RoF system under environmental variations, a temperature change was forced into the climatic chamber depicted in Fig. 2. The input RF power was then set to $P_{RF,IN} = -9\,dBm$, since this value determined an average EVM belonging to the interval of minimum for all the lengths considered. The EVM resulting from the transmission through the A-RoF link of the $800\,MHz$ LTE signal was monitored every 5 seconds for a total time of one hour. During this period the outage probability p_{outage_x} was computed, namely the percentage of time during which the threshold given by the LTE standard referred to the $x-QAM$ modulation format was overtaken. For better readability of the plots, the probability of compliance $p_{comp_x} = (1 - p_{outage_x})$ will actually be represented in the corresponding figures.

Figure 6 confirms the good performance of the A-RoF system for short ($L = 70\,m$) link lengths, as well as the not acceptable quality of the received signal for the length $L = 300\,m$. In correspondence to $L = 70\,m$, and to $L = 300\,m$, it was respectively computed $p_{comp,\,256} = 99.86\%$ and $p_{comp,\,256} = 0\%$.

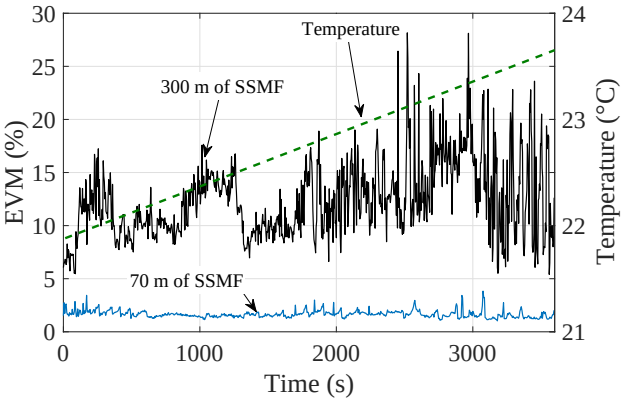

Fig. 6: Time measurement of EVM for $70\,m$ and for $300\,m$ of SSMF with $P_{RF,IN} = -9\,dBm$ at $800\,MHz$, utilizing the A-RoF link depicted in Fig. 2 with the symbolical switches S1 and S2 in positions A and C, respectively. This corresponds to the case in which only the SSMF is present along the link. The fiber has been inserted in the climatic chamber where the temperature changed with a linear ramp as indicated with the dashed line. The EVM was computed every 5 seconds within a total time interval of one hour.

IV. Performance of the A-RoF system in the proposed configuration

A. Comparison with the SSMF A-RoF system described in Section III

As already mentioned, the A-RoF system proposed in the present work corresponds to the one which results from Fig. 2 when the symbolical switches S1 and S2 are put in positions A and D, respectively, i.e. a short span of $\text{SMF}_{5\,\mu m}$ fiber is put before the G.652 fiber span. The main effect of this introduction is to excite within the G.652 fiber mostly the LP_{01} mode, reducing to a minimum the presence of the LP_{11} mode, and reducing consequently the combined effect of modal noise and intermodal dispersion as well.

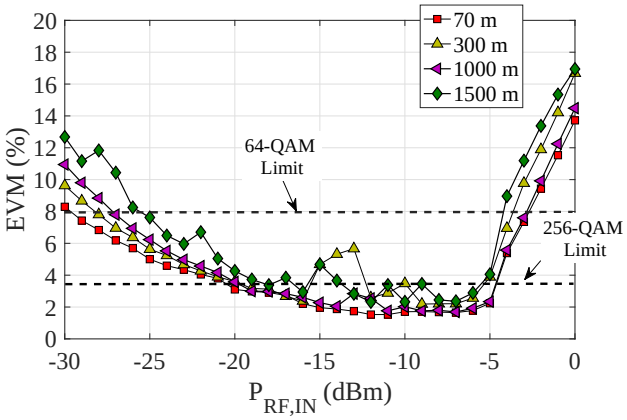

Fig. 7: EVM Measurements for all the distances considered inserting the $\text{SMF}_{5\mu m}$ before each SSMF span.

Figure 7 allows to appreciate that, excluding a little increase in the lower bound of $P_{RF,IN}$, due to the insertion loss of the $\text{SMF}_{5\,\mu m}$ patch, the performance of the links with $L = 70\,m$ (representative also for lower L values) and $L = 1\,km$ is substantially not changed. On the contrary, in the case when $L = 300\,m$ a great improvement can be observed, since a compliance with the LTE standard can be appreciated in almost all the range considered for $P_{RF,IN}$ at 64-QAM, and in the range $-12\,dBm \leq P_{RF,IN} \leq -5\,dBm$ at 256-QAM.

Similar considerations can be taken also for $L = 1.5\,km$, even if a less regular behavior seems to be present in this case with respect to the $L = 300\,m$ case. This is due to the fact that although the introduction of the $\text{SMF}_{5\,\mu m}$ patch leads to a reduction of the effects of intermodal dispersion and modal noise, fiber attenuation for $L = 1.5\,km$ (already taken into account in Fig. 4), and insertion loss of the $\text{SMF}_{5\,\mu m}$ patch reduce the signal to noise ratio to lower levels with respect to the $L = 300\,m$ case. Measurements performed over distances $L > 1.5\,km$ led to worse results, suggesting that $L \sim 1.5\,km$ can be taken as a reliable reference point for the upper limit of the MFH distances to be covered with the proposed system.

Referring now to the 1-hour monitoring of the received LTE signal under forced temperature variations, Figure 8 allows to appreciate the improvement generated by the insertion of the $\text{SMF}_{5\mu m}$ for $L = 300\,m$ and $f_c = 800\,MHz$. The value of the quantity $p_{comp,\,64}$ passed from 8% to 100%, while $p_{comp,\,256}$ passed from 0% to 89%.

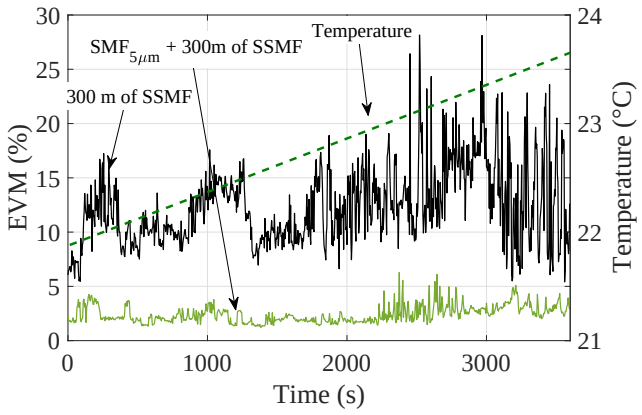

Fig. 8: Example of EVM time measurements for $300\,m$ of SSMF with $P_{RF,IN} = -9\,dBm$ at $800\,MHz$. Both cases in which the $\text{SMF}_{5\mu m}$ is present (green curve) and is not present (black curve) are shown. The temperature ramp is also indicated.

In line with what was observed above, for $L = 70\,m$ no particular performance variations were instead observed. Indeed, the values of $p_{comp,\,64}$ and $p_{comp,\,256}$ passed respectively from 100% and 99.86% to 100% and 100%.
As mentioned above, to better highlight the performance of the proposed A-RoF system for $L = 300\,m$, frequencies ranging in the interval $500\,MHz \leq f_c \leq 1\,GHz$ were considered. Figures 9a and 9b report respectively the mean value and the standard deviation of the measured EVM within such interval.

The improved performance of the proposed system can be appreciated at $800\,MHz$, where the mean EVM goes from 12.38% to 2.43%, and is maximum at $f_c = 700\,MHz$ where the value goes from 24.6% to less than 2.26%. Figure 9b highlights that the maximum improvement of σ_{EVM} is obtained for 700 MHz, passing from 16.75% to 0.68%, while for 800 MHz σ_{EVM} reduces from 3.59% to 0.8%. Figure 10 allows to appreciate the performance of the proposed A-RoF system in terms of $p_{comp,\,256}$. It can be noted that for 800 MHz $p_{comp,\,256}$ goes from 0% to 89%, while for 600 MHz it exhibits the greatest improvement, going from 0% to 99.86%. Qualitatively similar results have been found for $p_{comp,\,64}$, which reaches in the proposed case the value of 100% for all the frequencies considered.

Although the present analysis has been focalized on the case $L = 300\,m$, note that the concept on which the presented solution is based has a general applicability, and can therefore be successfully utilized within different sets of frequency intervals and short-medium range link lengths, as can be desumed from Fig. 4 reported above.

B. Comparison with GI-MMF A-RoF systems based on VCSELs

The purpose of this subsection is to give a whole view about the employment of $850\,nm$ VCSELs in A-RoF systems for short and medium range MFH applications. As mentioned in Section II, the performances of the SSMF-based RoF

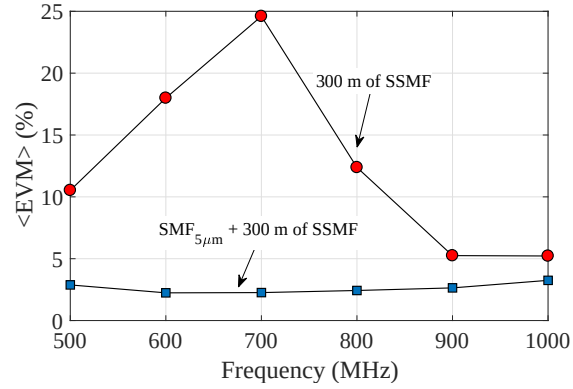

(a)

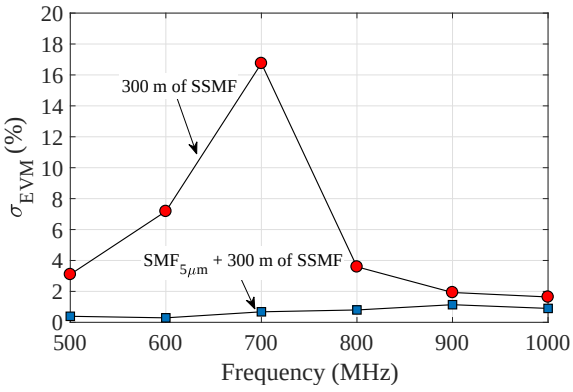

(b)

Fig. 9: (a) Average value of EVM for $L = 300\,m$ and $P_{RF,IN} = -9\,dBm$. The beneficial effect of inserting the $\text{SMF}_{5\mu m}$ patch is also shown. The same effect is shown for the EVM standard deviation (b).

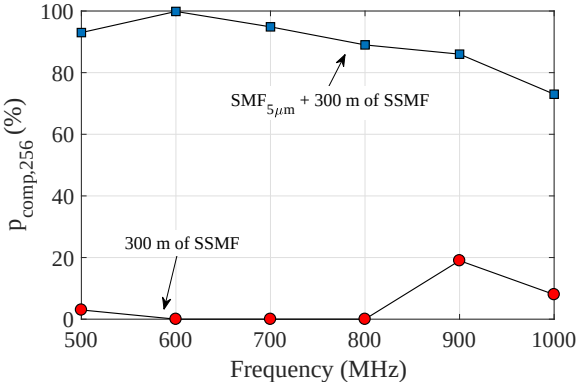

Fig. 10: The graph represents the outage probability for 256-QAM transmission without (circles) and with (squares) the insertion of the $\text{SMF}_{5\mu m}$.

system proposed have been compared with a system which employs the same SM VCSEL and GI-MMF instead of SSMF. Moreover, a further comparison using MTM VCSEL and GI-MMF is presented. The reason lies in the fact that the latter are common systems employed in several short-medium range telecommunication links.

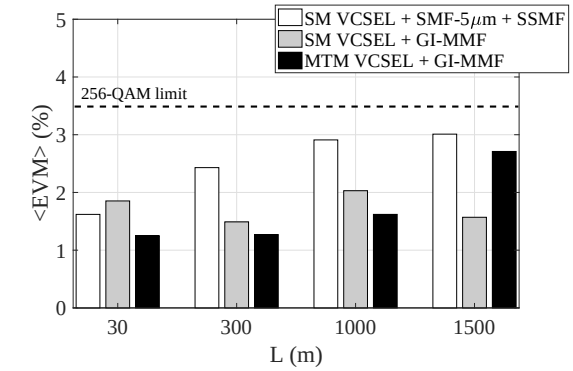

(a)

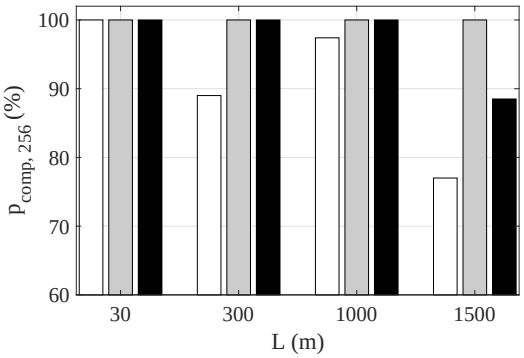

(b)

Fig. 11: Average EVM (a) and 256-QAM compliance probability (b) for RoF link based on SM VCSEL, $\text{SMF}_{5\mu m}$ and SSMF (white), SM VCSEL and GI-MMF (grey), MTM VCSEL and GI-MMF (black).

Figures 11a and 11b show the trend of average values of EVM and $p_{comp,256}$ for the three different systems considered varying the link distances. Note that, the $20\,MHz$ bandwidth LTE signal used in this work is the maximum admitted bandwidth for a single LTE channel. Indeed, due to the bandwidth size, this represents the worst case of Signal-to-Noise Ratio when a certain $P_{RF,IN}$ is fixed.

Focalizing initially on the two systems based on GI-MMF, it can be noted that they practically exhibit the same performance for $L \leq 1000\,m$. Indeed, the differences in the EVM values smaller than one percentage point can be easily met with either sign due to the not perfect reproducibility of the optical connections. However, for higher distances (such as $1500\,m$) the system composed by SM VCSEL + GI-MMF performs better than the one composed by MTM VCSEL + GI-MMF. This fact can be related to the effect of intermodal dispersion and chromatic dispersion which both become relevant in presence of multimode lasers such as the MTM VCSEL employed.

Note also that the proposed system (SM VCSEL + $\text{SMF}_{5\,\mu m}$+ SSMF) exhibits slightly lower performances with respect to the other two based on GI-MMF. This is due to the fact that the MTM and SM VCSELs were commercially designed to be efficiently coupled respectively with a GI-MMF and with a $9\,\mu m-$core SSMF (and consequently also with a GI-MMF). Therefore, while our proposed insertion of a smaller core diameter fiber (such as the $\text{SMF}_{5\,\mu m}$) right before the SSMF span gives the described advantages, it also produces an optical coupling loss, which increases the Noise Figure of few dB of the global system ending up in higher values of the average EVM/lower values of $p_{comp,256}$.

Indeed, the mis-coupling is not present in the other two cases where the VCSELs are directly coupled with fibers with diameter equal or higher than the one for which they are designed. As a matter of fact, a further margin of improvement in the performance of the proposed solution (SM VCSEL + $\text{SMF}_{5\,\mu m}$+ SSMF) can be reasonably envisaged, provided that a SM VCSEL source is utilized which features an optimized coupling with optical fibers with $5\,\mu m$ core diameter.

In this view from Figure 11a it can be concluded that the A-RoF system proposed allows the transmission of 256-QAM signals in compliance with the requirements of the LTE standard since the average value of EVM falls in all cases below the given upper limit. More in general, both Figures 11a and 11b demonstrate that the usage of G.652 fiber can lead to performances near to GI-MMF for both the quantities considered showing that the proposed solution can represent the optimal one in terms of performance to cost ratio in those cases where a SSMF infrastructure is already available.

V. Conclusion

The possibility of decreasing costs and consumption in the realization of Mobile Front-hauls in Very Dense Networks has been investigated through the employment of an A-RoF link based on $850\,nm$ single mode VCSELs and G.652 fiber. The feasibility of the system has been evaluated in terms of EVM and outage probability for a $20\,MHz$ LTE signal in band 20 of the standard (around $800\,MHz$). Despite the problems related to the bi-modal propagation in G.652 due to the operating wavelength of $850\,nm$, it has been shown that 256-QAM $20\,MHz$ LTE transmission, which corresponds to a raw data rate of 134.4 Mbit/s, is possible up to $1.5\,km$, while for low modulation bandwidth it is possible to achieve higher performances and/or distances. A final comparison among SSMF and GI-MMF using both SM and MTM VCSEL prove that the proposed system is able to reach the same performances, with the possibility of decreasing further the costs in case of an infrastructure based on G.652 fiber is already present in the area to be served.

References

[1] C. Liu, L. Zhang, M. Zhu, J. Wang, L. Cheng, and G. K. Chang, "A novel multi-service small-cell cloud radio access network for mobile backhaul and computing based on radio-over-fiber technologies," *J. Lightw. Technol.*, vol. 31, no. 17, pp. 2869–2875, Sept 2013.

[2] I. Chih-Lin and J. Huang, "RAN revolution with NGFI (xHaul) for 5G," in *Optical Fiber Commun. Conf. and Exhibition (OFC)*, March 2017, pp. 1–4.

[3] Cisco, "Cisco 5G Vision Series: Small Cell Evolution," Cisco, Tech. Rep., 2015.

[4] T. Pfeiffer, "Next generation mobile fronthaul and midhaul architectures [invited]," *IEEE/OSA J. Optical Commun. and Networking*, vol. 7, no. 11, pp. B38–B45, November 2015.

[5] NOKIA, "Ultra Dense Network (UDN) White Paper," NOKIA, Tech. Rep., 2016.

[6] Ericsson, Ed., *Ericsson Review: Connecting the dots: small cells shape up for high-performance indoor radio* , vol. 91, December 2014.

[7] D. Wake, A. Nkansah, and N. J. Gomes, "Radio Over Fiber Link Design for Next Generation Wireless Systems," *J. Lightw. Technol.*, vol. 28, no. 16, pp. 2456–2464, Aug 2010.

[8] N. J. Gomes, P. Assimakopoulos, M. K. Al-Hares, U. Habib, and S. Noor, "The new flexible mobile fronthaul: Digital or analog, or both?" in *18th Int. Conf. on Transparent Optical Networks (ICTON)*, July 2016, pp. 1–4.

[9] A. Pizzinat, P. Chanclou, T. Diallo, and F. Saliou, "Things you should know about fronthaul," in *The European Conf. on Optical Commun. (ECOC)*, Sept 2014, pp. 1–3.

[10] C.-T. Tsai, C.-H. Lin, C.-T. Lin, Y.-C. Chi, and G.-R. Lin, "60-GHz Millimeter-wave Over Fiber with Directly Modulated Dual-mode Laser Diode," *Sci. Rep.*, vol. 9, 2016.

[11] C. Y. Lin, Y. C. Chi, C. T. Tsai, H. Y. Wang, and G. R. Lin, "39-GHz Millimeter-Wave Carrier Generation in Dual-Mode Colorless Laser Diode for OFDM-MMWoF Transmission," *IEEE J. Sel. Topics Quantum Electron.*, vol. 21, no. 6, pp. 609–618, Nov 2015.

[12] P. Li, W. Pan, X. Zou, B. Lu, L. Yan, and B. Luo, "Image-free microwave photonic down-conversion approach for fiber-optic antenna remoting," *IEEE Journal of Quantum Electronics*, vol. 53, no. 4, pp. 1–8, Aug 2017.

[13] Z. Tayq, L. A. Neto, F. Saliou, C. A. Berthelemot, J. Gomes, T. Haustein, M. Lacouche, J. Plumecoq, L. Bellot, and P. Chanclou, "Real time demonstration of fronthaul transport over a mix of analog and digital rof," in *2017 19th International Conference on Transparent Optical Networks (ICTON)*, July 2017, pp. 1–4.

[14] V. A. Thomas, M. El-Hajjar, and L. Hanzo, "Performance Improvement and Cost Reduction Techniques for Radio Over Fiber Communications," *IEEE Commun. Surveys Tutorials*, vol. 17, no. 2, pp. 627–670, Secondquarter 2015.

[15] R. Michalzik, Ed., *VCSELs Fundamentals, Technology and Applications of Vertical-Cavity Surface-Emitting Lasers*. Springer, 2013.

[16] J. A. Tatum, D. Gazula, L. A. Graham, J. K. Guenter, R. H. Johnson, J. King, C. Kocot, G. D. Landry, I. Lyubomirsky, A. N. MacInnes, E. M. Shaw, K. Balemarthy, R. Shubochkin, D. Vaidya, M. Yan, and F. Tang, "VCSEL-Based Interconnects for Current and Future Data Centers," *J. Lightw. Technol.*, vol. 33, no. 4, pp. 727–732, Feb 2015.

[17] H.-Y. Kao *et al.*, "Comparison of single-/few-/multi-mode 850 nm vcsels for optical ofdm transmission," *Opt. Express*, vol. 25, no. 14, pp. 16 347–16 363, Jul 2017.

[18] C. T. Tsai *et al.*, "Multi-mode vcsel chip with high-indium-density ingaas/algaas quantum-well pairs for qam-ofdm in multi-mode fiber," *IEEE J. Quantum Electron.*, vol. PP, no. 99, pp. 1–1, 2017.

[19] R. Puerta, M. Agustin, . Chorchos, J. Toski, J. R. Kropp, N. Ledentsov, V. A. Shchukin, N. N. Ledentsov, R. Henker, I. T. Monroy, J. J. V. Olmos, and J. P. Turkiewicz, "Effective 100 gb/s im/dd 850-nm multi- and single-mode vcsel transmission through om4 mmf," *Journal of Lightwave Technology*, vol. 35, no. 3, pp. 423–429, Feb 2017.

[20] C. Carlsson, A. Larsson, and A. Alping, "Rf transmission over multimode fibers using vcsels-comparing standard and high-bandwidth multimode fibers," *J. of Lightwave Technology*, vol. 22, no. 7, pp. 1694–1700, July 2004.

[21] J. Guillory, A. Pizzinat, B. Charbonnier, and C. Algani, "60 GHz intermediate frequency over fiber using a passive multipoint-to-multipoint architecture," in *16th European Conf. on Networks and Optical Commun.*, July 2011, pp. 44–47.

[22] B. Elliot and M. Gilmore, *Fiber Optic Cabling*, 2nd ed., Newnes, Ed. Linacre House, Jordan Hill, Oxford: Newnes, 2002.

[23] D. Vez, S. G. Hunziker, R. Kohler, P. Royo, M. Moser, and W. Bachtold, "850 nm vertical-cavity laser pigtailed to standard singlemode fibre for radio over fibre transmission," *Electron. Lett.*, vol. 40, no. 19, pp. 1210–1211, Sept 2004.

[24] B. G. Kim, S. H. Bae, H. Kim, and Y. C. Chung, "Mobile fronthaul optical link for lte-a system using directly-modulated 1.5-μm vcsel," in *21st OptoElectronics and Commun. Conf. (OECC)/ Int. Conf. on Photonics in Switching (PS)*, July 2016, pp. 1–3.

[25] I. Papakonstantinou, S. Papadopoulos, C. Soos, J. Troska, F. Vasey, and P. Vichoudis, "Modal Dispersion Mitigation in Standard Single-Mode Fibers at 850 nm With Fiber Mode Filters," *IEEE Photonics Technol. Lett.*, vol. 22, no. 20, pp. 1476–1478, Oct 2010.

[26] J. Nanni, S. Rusticelli, C. Viana, J. L. Polleux, C. Algani, F. Perini, and G. Tartarini, "Modal Noise Mitigation in 850-nm VCSEL-Based Transmission Systems Over Single-Mode Fiber," *IEEE Trans. Microw. Theory Tech.*, vol. 64, no. 10, pp. 3342–3350, Oct 2016.

[27] J. Nanni, F. Pizzuti, J. Polleux, C. Algani, and G.Tartarini, "VCSEL-SSMF-based Radio-over-Fiber link for low cost and low consumption Wireless Dense Networks," in *Proc. Int. Topical Meeting Microw. Photonics (MWP)*, Beijing, China, October 2017.

[28] *LTE Evolved Universal Terrestrial Radio Access (E-UTRA)*, 3GPP Std., Rev. 13.

[29] U. Rehfuess, "5G for people and things,700 MHz band as key to success for wide area 5G services," NOKIA, Tech. Rep., 2017.

[30] J. Nanni *et al.*, "Modal noise in 850nm VCSEL-based radio over fiber systems for manifold applications," in *Fotonica AEIT Italian Conf. Photonics Technologies*, Turin, Italy, May 2015, pp. 1–4.

[31] *LTE Evolved Universal Terrestrial Radio Access (E-UTRA); Base Station (BS) radio transmission and reception*, 3GPP Std., Rev. 11.